POLITECNICO DI TORINO
Repository ISTITUZIONALE

Techniques and Survey for 3D Modeling of Touristic Caves: Valdemino Case

Original
Techniques and Survey for 3D Modeling of Touristic Caves: Valdemino Case / Pisoni, I.N., Cina, A., Grasso, N., Maschio, P.F. - In: Communications in Computer and Information ScienceELETTRONICO. - [s.l] : Springer, Cham, 2022. - ISBN 978-3-031-17439-1. - pp. 317-328 [10.1007/978-3-031-17439-1_23]

Availability:
This version is available at: 11583/2973281 since: 2022-11-22T13:08:31Z

Publisher:
Springer, Cham

Published
DOI:10.1007/978-3-031-17439-1_23

Terms of use:

This article is made available under terms and conditions as specified in the corresponding bibliographic description in the repository

Publisher copyright

(Article begins on next page)

11 September 2026

Techniques and Survey for 3D Modeling of Touristic Caves: Valdemino Case

Isabella Nicole Pisoni(✉), Alberto Cina, Nives Grasso, and Paolo Maschio

DIATI - Department of Environmental, Land and Infrastructure Engineering, Politecnico di Torino, Corso Duca degli Abruzzi 24, 10129 Torino, Italy
{isabella.pisoni,alberto.cina,nives.grasso,
paolo.maschio}@polito.it

Abstract. Nowadays, touristic caves are a relevant topic among topographical and geological studies. Modern techniques allow to elaborate 3D models with high accuracy and precision. Anyway, underground surveys are always delicate to perform, due to narrow and difficult to reach environments. In this paper, we show a case study, "Valdemino" cave, that involved the utilization of different point cloud acquisition methods: UAV, TLS, SLAM. The first purpose was to obtain 3D models of outdoor and indoor environments with a medium and high accuracy. These models were used to calculate the thickness of the rock between surface and cave's roof and will be used for further studies, taking part in the PRIN 2017 project, concerning the impact of the tourist on show caves. The second purpose was to discuss about the feasibility and precision of the different survey methods, when studying a cave. The results showed how SLAM technology is enough accurate for speleological purposes, if compared with the more accurate TLS method. It is precise, maneuverable, easy to use and it allowed to get into environments that TLS can't reach, such as non-touristic areas.

Keywords: SLAM technology · Touristic cave · UAV acquisition · LiDAR technology · Underground survey · 3D modeling

1 Introduction

In the last decades, a particular attention has been raised on touristic caves and the impact of human presence on the equilibrium of these delicate environments [1–4]. The contribute of geomatics has become really significant, with the implementation of various 3D mapping methods [5–8]. 3D modeling can be used for a lot of different purposes that range from tourism to risks assessment.

Terrestrial laser scanners (TLS) have been widely used to map outdoor environments and even caves [9], but underground and indoor surveys are a critical case, since instruments whose acquisitions are realized with marker surveyed by GNSS (Global Navigation Satellite System) and total station, such as TLS, are hard to use, due to difficult operating conditions [10]. That's why it is necessary to use them together with topographical instruments, that measure angles and distances, for example total stations

© The Author(s) 2022
E. Borgogno-Mondino and P. Zamperlin (Eds.): ASITA 2022, CCIS 1651, pp. 317–328, 2022.
https://doi.org/10.1007/978-3-031-17439-1_23

[11]. This way, a geodetic traverse is built and TLS are placed over points with known coordinates. Anyway, it happens that underground areas are not easily accessible and therefore not suitable for TLS. In these cases, some other instruments can be used, starting from SLAM (Simultaneous Localization And Mapping) based portable instruments, for example [5, 6, 12]. They are equipped with Distance Measuring Instruments (DMI), profilers, Inertial Measurement Units (IMU) and sometimes with camera sensors. They are portable, maneuverable and they can be placed on a backpack or handheld. They don't need to be constantly geo-referenced during acquisition, because point clouds are built over trajectories calculated by algorithms based on image navigation integrated with IMU [13, 14].

In this paper we show a case study, "Valdemino Cave" in Borgio Verezzi, where we have studied and compared some geomatic techniques in very difficult and extreme environment. The purpose is to give support and analysis of environmental sustainability of touristic caves.

We adopted two different approaches for data acquisition. The first one consisted in using a Teledyne Optech Polaris (a TLS) and a total station, the second one using a KAARTA Stencil 2 (SLAM technology based). For indoor surveys, in fact, there is often the need to compare and integrate different systems to get more complete data and to verify the precision of each technique with respect to the others [12, 15]. In this case study, we used TLS method as reference for the other one.

Evaluating the impact of the tourist in show caves means also studying the impact of urbanization around the cave's territory. The cave has to be considered as what it is: cavity underground, lying among urbanized areas, maybe with houses or that are going to host new buildings in the immediate future. In fact, one of the main purposes of this study is to investigate the thickness of the rock lying upon the cave's roof.

Modern photogrammetry techniques are a consolidated technique in many fields of environmental monitoring and surveys [16–19]. For our study, an unmanned aerial vehicle (UAV) DJI Phantom 4 aircraft was used to carry a camera in order to acquire images of the outside area surrounding the cave. Images have been later elaborated to get a 3D model of the surface and a digital elevation model (DEM). The photogrammetric model has been integrated with 3D underground model. We analyzed the accuracy of photogrammetric flight 3D model and Stencil 2 with respect to a traditional LiDAR (Light Detection And Ranging).

The products we obtained from this study consist in: dense clouds, orthomosaic images and DEM images.

1.1 Case Study

The Valdemino cave is situated on Borgio Verezzi territory, in Liguria region (Italy). Coordinates of the entrance: latitude 44°09′45" N, longitude 8°18′15" E. It's around 500 m distant from the sea and its elevation is a few meters above sea level, starting from 30 m at the entrance and lowering up to 2 m in correspondence to the last room.

Our study is part of the PRIN 2017 project about the impact of the tourist on show caves: "Progetto PRIN 2017: SHOWCAVE: a multidisciplinary research project to study, classify and mitigate the environmental impact in tourist caves".

2 Materials and Methods

This research is based on four essential parts: UAV based data acquisition with a DJI Phantom 4 aircraft for 3D terrain model, terrestrial laser scanner (TLS) and portable laser scanner LiDAR (PLS) data acquisition, data processing, DEMs and 3D models realization and analysis.

TLS acquisition was carried out after topographical measurements to build a geodetic traverse. In discussion we analyze and compare results and accuracy of different techniques.

2.1 UAV Based Data Acquisition and Processing

The very first step was to realize a manual flight embracing an area approximatively corresponding to the extension of the underground cave (about 5,5 ha). For this purpose, a DJI Phantom 4 aircraft was used, equipped with a GNSS receiver able to acquire RTK (Real Time Kinematic) corrections; the fix ambiguity phase allowed centimetric accuracy. Coordinates acquired belong to the projection centers, with centimetric accuracy, used for geo-localization and 3D model elaboration. On the drone, a gimbal camera, whose specifics are reported in Table 1, was placed. This camera can be oriented in different directions with different angles, up to 90°. Moreover, five markers were placed and detected their position with RTK GNSS (accuracy of a few cm). Three hundred-ninety-six nadir pictures were taken during the flight.

Table 1. Camera parameters.

Camera model	Ground resolution GSD	Focal length	Pixel size	Average height from the ground	Average scale
FC6310R 12 MP × 1″ sensor	1.32 cm/pix	8.8 mm	2.4 × 2.4 μm	48 m	5400

Data processing was realized through proprietary software AgiSoft Metashape [20]. For this study, we decided to try three different geo-localization approaches to estimate the variations in calibration parameters and distortion plot, involved in photos alignment and camera optimization. In the three different approaches we tried different combinations of GCPs (Ground Control Point), and CPs (Check Points), always using all the PCs (projection center) we had. We used the three approaches to evaluate the differences between the different solutions and to evaluate the importance of GCPs in the accuracy and estimation of the camera calibration. In Table 2 a resume of the three different cases.

After that, we elaborated different products: dense cloud, tiled model, orthomosaic, DEM. A particular attention was dedicated to DEM. Since one of the main aims of this study is to investigate the thickness of the rock lying between the surface and the roof of the cave, we actually needed a DTM. For this purpose, a classification was

Table 2. GCPs, CPs and PCs utilisation in the three different cases.

Case	GCP	CP	PC
1	5	0	396
2	1	4	396
3	0	5	396

realized. This procedure consisted in taking the dense cloud, selecting the groups of points corresponding to trees or houses by manually drawing polygonal contours around those elements and assigning them to two different classes, in this case respectively *trees* (green) and *buildings* (red). All the other points remained into class *ground*, as default. From here, we built a mesh using ground points only, obtaining a DTM. In Fig. 1, the classification is shown.

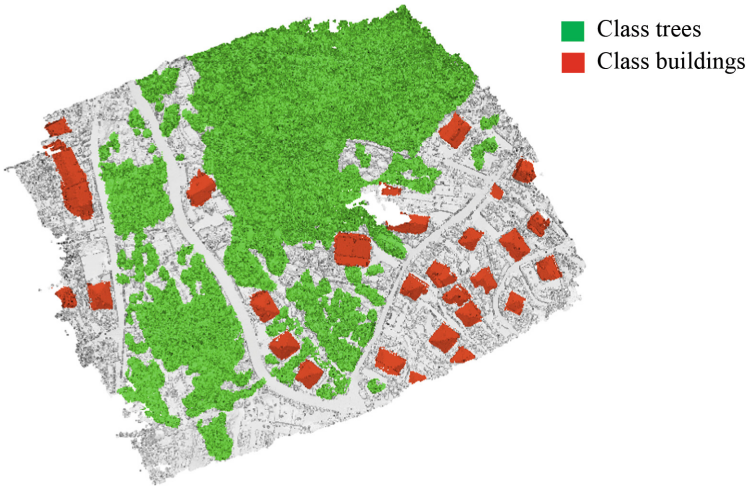

Fig. 1. Manual classification of dense cloud's points.

2.2 TLS Methodology, Acquisition and Processing

We used a Teledyne Optech Polaris (see Fig. 2a) for the acquisition of the reference point cloud of the indoor of the cave. This instrument is equipped with integrated sensors, such as internal L1 GNSS, inclination compensator, compass, camera controls and with external camera imaging system, a Nikon with a resolution of 24 MPx. It has a really wide acquisition range (up to 2000 m) and a high resolution (up to 1 mm at 33 m). The acquisition field of view is adjustable and reaches 360° [21]. Its specifics make it suitable for all kinds of environments but can have some limitation for caves, for example, due to the narrow indoor spaces.

The Polaris laser scanner allows to acquire point clouds directly georeferenced from a station point and an orientation point, starting from three points outside the cave and we built a geodetic traverse using a total station Leica MS50. With this method, we managed to place some points with extrapolated coordinates inside the cave, for a total of fifteen points, that have been used to place the Polaris for acquisition, directly georeferencing with targets on known points.

Data processing was realized using proprietary software Polaris ATLAScan [22]. We had fifteen separate directly georeferenced point clouds to be imported and elaborated, one for each scan. It was necessary to operate alignment; the majority of the clouds were already correctly oriented in space, since geo-referenced, but two appeared to be inclined with respect to the horizontal and needed to be corrected. When every scan was processed, we merged all the point clouds in a single one and colorized it, using internal camera pictures.

In the end, we exported a DEM, to have the elevation of the roof of the cave (the highest points detected during acquisition with TLS). DEM's resolution is 5 cm/pix.

2.3 SLAM Methodology, Acquisition and Processing

Slam method was applied using a KAARTA Stencil 2 (Fig. 2b). This instrument is composed by a Velodyne VLP-16, a MEMS (Micro Electronic Mechanical System) inertial platform and a feature tracker camera, connected to a processor Intel Core i7. The measuring procedure puts together LiDAR point acquisition and information from the feature tracker system, estimating motion where instrument is held.

This method is particularly suitable for caves because it allows to acquire points in small and narrow environments, since the instrument range goes from 10 cm up to 100 m, and it doesn't necessarily need a GNSS positioning (even if it can be integrated with). In fact, the instrument registers translational and rotational movement, registering a point cloud based on the trajectory of acquisition. Data processing integrates motion estimation, laser point acquisition and speed information to register acquired points in a local reference system. Then, with a mapping algorithm, similar geometric features are detected, to recognize coincident points in the point cloud [23].

KAARTA Stencil 2 is a relatively small and light instrument; it can be transported by hand or placed on a backpack. In this case study, we at first put it on a small handheld pole and then on a small backpack, in order to move easily inside the cave.

We performed several loop closed acquisitions. A first one covered the whole touristic path. We started and ended at the main entrance of the cave. The other acquisitions were taken along the non-touristic areas, considering the same room inside the cave as reference for starting point and ending point. In fact, we have placed particular attention to start and end at the same point, in order to operate loop closure and recognize later, during data elaboration, common areas in different acquisitions. Lastly, it was really important to have a minimum overlap between two or more scans, to allow post-processing registration activity.

A specific tool allows to simulate the acquisition process with a lower speed, changing some parameters characterizing the surveyed scene, to improve the trajectory estimation and the point cloud registration. Then, we performed loop closure for each acquisition. This allowed to force the overlap of the initial point with the ending point and it's really

important because sometimes the inertial-odometry system fails in registering correctly angles and directions, making the trajectory deviate from the real one, causing a shift between starting point and ending point, that should be the same [24].

After having all the scans cleaned and given a correct trajectory, we had to assign them coordinates. For this task, we used an open source software: Cloud Compare [25]. It has a specific tool that allows to align and orientate a point cloud using another one as reference, taking common points between the two. So, we imported the point cloud from ATLAScan software (that, for practical reasons we are going to call Polaris Cloud from now on) to be the reference. Fifteen common points between the two clouds were used, all of them with a residual error < 1 m. After registration, we performed the algorithm called Iterative Closest Point (ICP) that allows an even more precise registration of the two models [26], to optimize the result. The final global error after ICP was 43 cm. In the end, we calculated the distance cloud-to-cloud, between Polaris Cloud and the Cloud registered with Stencil 2 acquired in touristic path. We remind that we used Polaris Cloud as a reference, to evaluate the accuracy of Stencil 2 acquisition method.

Once we had assigned coordinates to the main cloud (the touristic path), we could merge it with the other point clouds, non-touristic areas, using the align tool and merging all the clouds as one (that we'll call KAARTA Cloud).

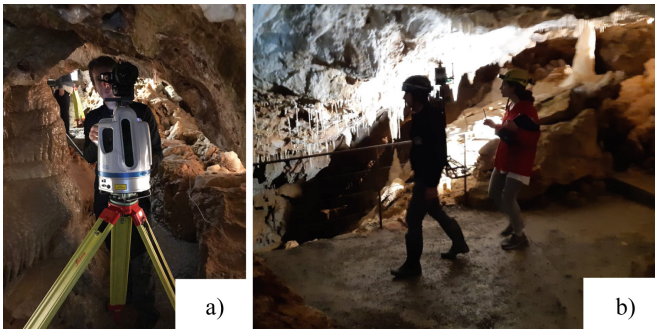

Fig. 2. a) Teledyne Optec Polaris. b). KAARTA Stencil 2.

3 Obtained Results

3.1 UAV Modeling

The first important result involves camera calibration and the role of the GCP. As said previously, three different cases were analyzed. For each case, camera calibration parameters and the distortion plot were analyzed (see Table 2). We expected to get at least a small difference between the three cases, since we thought that placing GCPs would have had an important influence on the geo-localization. The difference both in the calibration parameters and in the distortion plot of the three separate cases was actually really small. As an example, some calibration parameters in the three different cases are reported in

Table 3. Camera internal orientation and distortion coefficients.

Case	F [pixel]	Cx [pixel]	Cy [pixel]	K1	K2	K3
1	3628.78 ± 0.11	−2.39 ± 0.09	5.87 ± 0.09	0.006 ± 7.2E-5	−0.05 ± 3.5E-4	0.09 ± 6.6E-4
2	3631.99 ± 0.10	−2.94 ± 0.05	5.79 ± 0.10	0.006 ± 2.7E-5	−0.05 ± 1.2E-4	0.09 ± 2.3E-4
3	3634.15 ± 0.15	−3.41 ± 0.06	3.83 ± 0.14	0.006 ± 2.7E-5	−0.05 ± 1.2E-4	0.09 ± 2.3E-4

Table 3: we consider only the contribution of the radial distortion (coefficients K). The tangential distortion was negligible.

We plotted two curves representing the difference between distortion plots (Fig. 3).

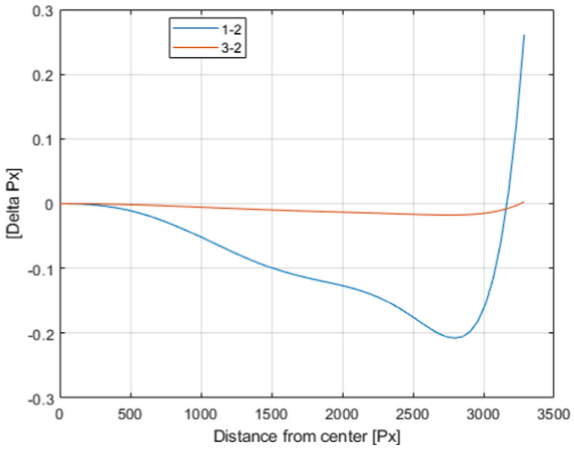

Fig. 3. Curves representing the difference between distortion plots of case 1 and case 2 (blue) and between distortion plots of case 3 and case 2 (red). Color figure online.

Taking case 2 as reference, we can observe that case 3 (0 GCP) and case 2 (1 GCP) have a difference almost equal to zero. On the contrary, case 1 (5 GCP) and case 2 have distortion plots that reach a difference of 0.3 Px.

Lastly, the final RMSE (root mean square deviation) for each case is pretty low (<10 cm), absolutely adequate for our purpose. Comparing the three cases, we could see how markers weren't strictly necessary, since the precision of geo-localization is guaranteed even with only the image acquisition centers: RTK projection centers.

If the camera calibration parameter and distortion plot of the three cases happened to be really similar in the three cases (showed in Table 3), a difference in the final RMSE (of GCPs, CPs and PCs) was observed. In Table 4 a resume.

GCPs appear not to be strictly necessary, since we obtained a centimetric accuracy even without them. Anyway, we noticed how the presence of even one GCP (case 2) decrease systematic effects obtained with only PCs (case 3); in fact, residuals on CPs get halved (8.7 ➔ 4.8 cm).

Table 4. Total 3D RMSE (cm) of residuals.

Case	GCP	CP	PC
1	2.2	–	1.6
2	6.2	4.8	2.9
3	–	8.7	2.1

3.2 Point Cloud Comparison

We had three different point clouds: drone photogrammetric model, 215.550.150 points, LiDAR Polaris Cloud (see Fig. 4a)), 150.158.080 points and KAARTA Cloud (see Fig. 4a)), 170.045.643 points. KAARTA Cloud (Fig. 4a)) covers a wider area than Polaris Cloud (Fig. 4b)) because with KAARTA Stencil 2 we could survey in part of the non-touristic path, too hard to survey with Polaris.

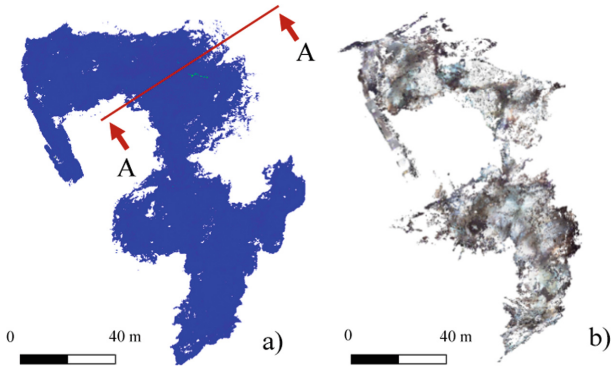

Fig. 4. a) and b) top view of Polaris Cloud (4a) and top view of KAARTA Cloud (4b).

When overlapping the point clouds, we observed that the RMSE after the alignment and the ICP is 0.43 m, that is acceptable for the speleological purpose of our study. Next step was to compare the external area and the cave, from now on using KAARTA Cloud. With Cloud Compare tools, we took some sections to examine the thickness of the rock along the area, that corresponds to the distance between surface cloud and KAARTA Cloud (example in Fig. 5).

Moreover, we imported the DTM from ATLAScan and the DTM from Metashape in QGIS [27], with a resolution of 5 cm/pix. With a difference between the second and the first, we obtained another DTM: thickness of the rock (see Fig. 6b)). On this DTM we could visualize the geodetic traverse built inside the cave, with its ellipses of error with 95% of probability (see Fig. 6a)).

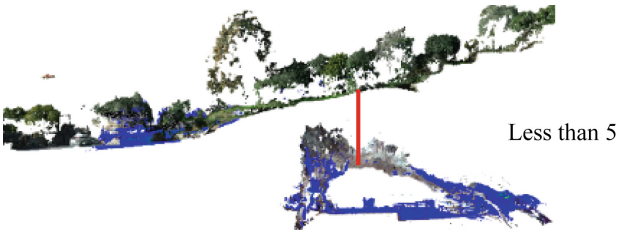

Fig. 5. Section A-A of the surface and the cave in correspondence of the first room. The red line shows the area where the thickness of the rock is the smallest.

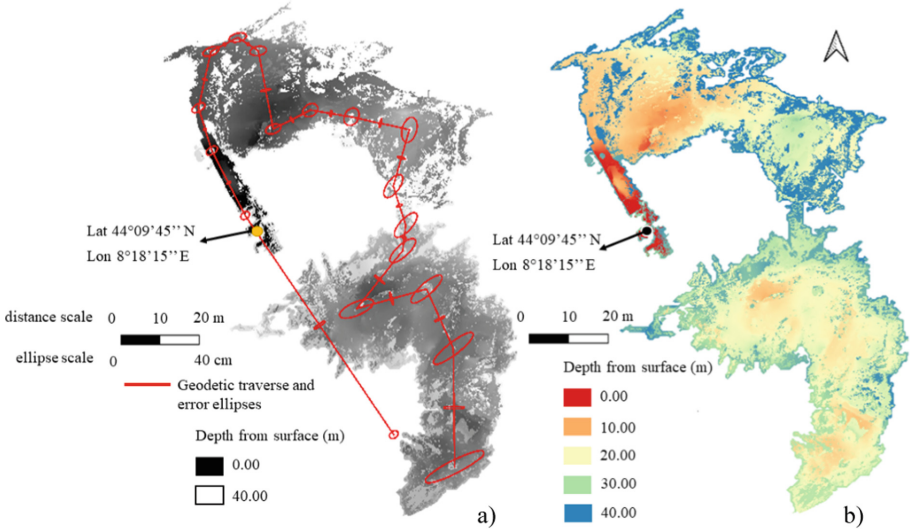

Fig. 6. a). DTM: difference between the classified DTM of the surface and the DTM of the cave, greyscale, with geodetic traverse and error ellipses, enhanced dimension by factor 50. b) DTM: difference between the classified DTM of the surface and the DTM of the cave, colorscale.

4 Discussion

4.1 Point Cloud

We said that the RMSE after KAARTA Cloud to Polaris Cloud registration is 0.43 m. In Fig. 7b) is shown the gaussian curve (in grey color) related to the distance between Polaris Cloud and KAARTA Cloud (colored histogram) in one particular selection of area (see Fig. 7a)), where the majority of the points see an average distance cloud-to-cloud lower than 24 cm. So, for our purposes, SLAM method can for sure be a valid substitute for static LiDAR technology, comporting a saving of time and a higher flexibility to move inside narrow environments. In Fig. 4a) and b), we can see how KAARTA Cloud has actually some parts more than Polaris Cloud. That's because with KAARTA Stencil 2 we managed to address more narrow environments, in addition to the touristic path. That made KAARTA Cloud more complete.

From the DTM showed in Fig. 6a), we could identify one particular critical point, that corresponds to the first big room of the cave and that can be seen also in section represented in Fig. 4. Here, the thickness of the rock appears to be less than 5 m; this has to be considered in case there is the need to build in correspondence of the area. The deepest roof point of the cave is approximatively at 21 m depth.

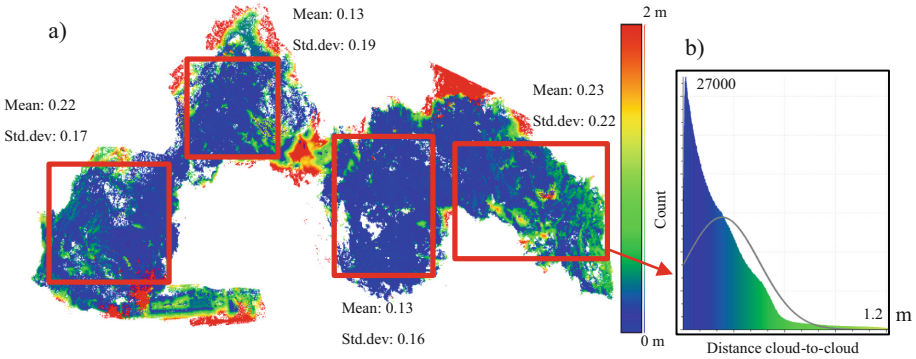

Fig. 7. a). Distance cloud-to-cloud in the entire area. Some captions were taken to verify the mean distance and the standard deviation. b). Histogram (coloured) and gaussian curve representing the distribution of absolute distance cloud-to-cloud between points belonging to KAARTA Cloud and points belonging to Polaris Cloud in one section of the entire area. On the x-axis: cloud-to-cloud distance, on the y-axis, count of points with a corresponding distance cloud-to-cloud. We can generally estimate the accuracy as a weighted average of the 4 cases: it results 17 ± 3 cm.

Lastly, since the point cloud are geo-localized, every single point has coordinates. This is very useful to investigate the disposition of conformations of interest inside the cave and in particular the water level. In fact, Polaris Cloud is so detailed and precise that shows the presence of water in some of the rooms of the cave. Even if laser scanner doesn't actually work for water (the signal is not reflected), some light blue color is detected, together with the presence of a clear horizontal line where the surface of the cave seems to be cut, that corresponds to water level.

5 Conclusions

In this case study, two different laser scanner acquisition techniques have been compared. Teledyne Optec Polaris, a TLS and KAARTA Stencil 2, a SLAM technology-based laser scanner. Both the techniques appeared to be precise and correct enough for the purpose of building a 3D model of the cave but SLAM technology resulted to be more practical and more suitable to map really narrow environments, where TLS can't reach. In fact, it allowed to register a wider area of the cave, including also non-touristic paths, without the need of a GNSS localization during acquisition. Moreover, while TLS acquisition took two days to be concluded, with KAARTA Stencil 2 we needed just a few hours to complete our tour. Anyway, Teledyne Optec Polaris for sure was useful to determine the accuracy of KAARTA Stencil 2 acquisition and processing.

The 3D models obtained are so accurate, that could be implemented as a virtual reproduction of the indoor area of the cave. The accuracy can be estimated from the comparison with respect to the reference cloud (Polaris) and is equal to 17 cm.

Then, thanks to 3D modeling of the surface, through UAV based method, we managed to get an approximation of the thickness of the rock lying between the surface and the roof of the cave, comparing two different DEMs.

Fundings and Acknowledgments. Progetto PRIN 2017: SHOWCAVE: a multidisciplinary research project to study, classify and mitigate the environmental impact in tourist caves.

Particular thanks to Professors Bartolomeo Vigna and Engineer Valentina Balestra. Special thanks also to Professors Marco Isaia and Rossana Bellopede, coordinators of the project PRIN 2017.

References

1. Calaforra, J.M., et al.: Environmental control for determining human impact and permanent visitor capacity in a potential show cave before tourist use. Environ. Conserv. **30**(2), 160–167 (2003)
2. Constantin, S., et al.: Monitoring human impact in show caves. A study of four Romanian caves. Sustainability **13**(4), 1619 (2021)
3. Mulec, J.: Human impact on underground cultural and natural heritage sites, biological parameters of monitoring and remediation actions for insensitive surfaces: case of Slovenian show caves. J. Nat. Conserv. **22**(2), 132–141 (2014)
4. Balestra, V., et al.: Study of the environmental impact in show caves: a multidisciplinary research. Geoingegneria Ambientale e Mineraria, Anno LVIII, n. II-III, dicembre **163–164**, 24–35 (2021). https://doi.org/10.19199/2021.163-164.1121-9041.024
5. Daniele, G., et al.: Survey solutions for 3D acquisition and representation of artificial and natural caves. Appl. Sci. **11**(14), 6482 (2021)
6. Sammartano, G., Spanò, A.: Point clouds by SLAMbased mobile mapping systems: accuracy and geometric content validation in multisensor survey and stand-alone acquisition. Appl. Geomatics **10**(4), 317–339 (2018)
7. De Waele, J., Fabbri, S., Santagata, T., Chiarini, V., Columbu, A., Pisani, L.: Geomorphological and speleogenetical observations using terrestrial laser scanning and 3D photogrammetry in a gypsum cave (Emilia Romagna, N. Italy). Geomorphology **319**, 47–61 (2018)
8. Weinmann, M.: Reconstruction and Analysis of 3D Scenes. Springer, Cham (2016). https://doi.org/10.1007/978-3-319-29246-5
9. Mohammed Oludare, I., Pradhan, B.: A decade of modern cave surveying with terrestrial laser scanning: a review of sensors, method and application development. Int. J. Speleol. **45**, 8 (2016)
10. Kang, Z., Yang, J., Yang, Z., Cheng, S.: A review of techniques for 3d reconstruction of indoor environments. ISPRS Int. J. Geo-Inf. **9**, 330 (2020)
11. Keller, F., Sternberg, H.: Multi-sensor platform for indoor mobile mapping: system calibration and using a total station for indoor applications. Remote Sens. **5**(11), 5805–5824 (2013)
12. Lagüela, S., Dorado, I., Gesto, M., Arias, P., González-Aguilera, D., Lorenzo, H.: Behavior analysis of novel wearable indoor mapping system based on 3D-SLAM. Sensors **18**, 766 (2018)

13. Dissanayake, M.G., Newman, P., Clark, S., Durrant-Whyte, H.F., Csorba, M.: A solution to the simultaneous localization and map building (SLAM) problem. IEEE Trans. Robot. Autom. **17**(3), 229–241 (2001)
14. Zhang, J., Singh, S.: Laser–visual–inertial odometry and mapping with high robustness and low drift. J. Field. Robot. **35**(8), 1242–1264 (2018)
15. Chiabrando, F., Della Colletta, C., Sammartano, G., Spanò, A., Spreafico, A.: Torino 1911 project: a contribution of a slam-based survey to extensive 3D heritage modeling. Int. Arch. Photogrammetry. Remote. Sens. Spat. Inf. Sci. **XLII-2**, 225–234 (2018). https://doi.org/10.5194/isprs-archives-XLII-2-225-2018
16. Elena, B., et al.: Precision agriculture workflow, from data collection to data management using FOSS tools: an application in northern Italy vineyard. ISPRS Int. J. Geo. Inf. **10**(4), 236 (2021)
17. Marco, P., et al.: Multi-temporal study of BELVEDERE glacier for hydrologic hazard monitoring and water resource estimation using UAV: tests and first results. IN:EGU General Assembly Conference Abstracts (2016)
18. Piras, M., Di Pietra, V., Visintini, D.: 3D modeling of industrial heritage building using COTSs system: test, limits and performances. Int. Arch. Photogrammetry. Remote Sens. Spat. Inf. Sci. **42**, 281 (2017)
19. Nex, F., Remondino, F.: UAV for 3D mapping applications: a review. Appl. Geomatics **6**(1), 1–15 (2013). https://doi.org/10.1007/s12518-013-0120-x
20. Agisoft Metashape Professional. www.agisoft.com. Version 1.8.2 build 14127 (64 bit) (2022)
21. Teledyneoptec Homepage. www.teledyneoptech.com/en/products/static-3d-survey/polaris/. Accessed 11 Mar 2021
22. Teledyne Optec, 2021, ATLAScan Version 1.2.10
23. Kaarta, Kaarta, Instructions for Stencil® (2018)
24. Williams, B., Cummins, M., Neira, J., Newman, P., Reid, I., Tardós, J.: A comparison of loop closing techniques in monocular SLAM. Robot. Auton. Syst. **57**, 1188–1197 (2009)
25. Cloud Compare. www.cloudcompare.org. 2022, Version 2.11.3 (Anoia)
26. Dabove, P., Grasso, N., Piras, M.: Smartphone-based photogrammetry for the 3D modeling of a geomorphological structure. Appl. Sci. **9**(18), 3884 (2019)
27. QGIS GNU General Public License. www.gnu.org. 2022, Version 3.16.1-Hannover

Open Access This chapter is licensed under the terms of the Creative Commons Attribution 4.0 International License (http://creativecommons.org/licenses/by/4.0/), which permits use, sharing, adaptation, distribution and reproduction in any medium or format, as long as you give appropriate credit to the original author(s) and the source, provide a link to the Creative Commons license and indicate if changes were made.

The images or other third party material in this chapter are included in the chapter's Creative Commons license, unless indicated otherwise in a credit line to the material. If material is not included in the chapter's Creative Commons license and your intended use is not permitted by statutory regulation or exceeds the permitted use, you will need to obtain permission directly from the copyright holder.